

# Time-resolved spectra of a self-pulsing quantum dot laser

A. Tierno, N. Radwell, T. Ackemann

SUPA and Department of Physics, University of Strathclyde, Glasgow G4 ONG, Scotland, UK

A. Tierno, N. Radwell, T. Ackemann. "Time-resolved spectra of a self-pulsing quantum dot laser." *Semiconductor Lasers and Laser Dynamics IV*, K. Panajotov, M. Sciamanna, A. A. Valle, R. Michalzik (editors). Proc. SPIE **7720**, 77202H, 2010.

Copyright 2010 Society of Photo-Optical Instrumentation Engineers. One print or electronic copy may be made for personal use only. Systematic reproduction and distribution, duplication of any material in this paper for a fee or for commercial purposes, or modification of the content of the paper are prohibited.

<http://dx.doi.org/10.1117/12.863582>

## ABSTRACT

Self-sustained pulsations in the output of an InAs quantum dot laser diode in the MHz range are reported for the first time. The characteristics (shape, range and frequency) are presented for the free running laser and when optical feedback in the Littrow configuration is applied. The frequency resolved optical spectra reveal different envelope shifts between the two cases. This might be related to a change of phase-amplitude coupling across the gain maximum in agreement with the expectation for a two level system. The time scale and bifurcation scenario suggest that these are opto-thermal pulsation like those reported in quantum well amplifiers.<sup>1</sup>

**Keywords:** quantum dot laser, self-pulsing, opto-thermal pulsations.

## 1. INTRODUCTION

Quantum dots (QD) lasers and amplifiers are emerging as an attractive light source in the wavelength range between 1.2-1.3  $\mu\text{m}$  and it is important to assess their performance and stability (for a recent overview of the field see, e.g., the contributions in the special issues<sup>2</sup> and<sup>3</sup>). One subject of interest are self-pulsing lasers where self-Q-switching due to saturable absorption was observed in many devices.<sup>4-7</sup> Pulsations are in the GHz region as can be expected for passive Q-switching with the lifetime of the excited state in the nanosecond range. In VCSELs, self-pulsations observed were at a somewhat lower frequency but still in the several hundreds of MHz range and were related to saturable absorption in lateral unpumped regions of the device.<sup>8</sup> Self-pulsations in edge-emitting QD lasers without an intentionally introduced absorber section were also observed and explained in terms of the inhomogeneous nature of the QD gain, the existence of several confined QD states and the resulting saturable absorption by energy states lower than the laser photon energy.<sup>9</sup> Nevertheless, these oscillations are still in the GHz range.

We are reporting here on self-pulsations in QD edge-emitting lasers without a saturable absorber section taking place on the MHz scale. The oscillation frequency as well as the square-wave shape hint to a thermal origin of the dynamics. Indeed, opto-thermal pulsations with a very similar phenomenology were studied in quantum well amplifiers<sup>1,10</sup> and are typical for a variety of other nonlinear optical systems.<sup>11-14</sup> It was shown in<sup>1</sup> that the self-oscillations follow van der Pol-Fitzhugh-Nagumo dynamics,<sup>15,16</sup> a fairly general scenario of relaxation oscillations, which are characterized by the competition of very different time scales (in<sup>4,10</sup> for example carrier dynamics and thermal relaxation).

Interestingly, the self-pulsing dynamics are found to persist if frequency-selective feedback is applied. By the feedback, the operation frequency of the laser can be tuned above, below and around gain maximum and time-resolved optical spectra show characteristic differences, which are argued to give some indication of a difference in phase-amplitude coupling above and below the gain maximum.

---

Further author information: corresponding email: [thorsten.ackemann@strath.ac.uk](mailto:thorsten.ackemann@strath.ac.uk)

## 2. DEVICES AND EXPERIMENTAL SETUP

The laser is an edge-emitting diode (QDL) from Innolume GmbH with a length of  $L = 3.5$  mm. It contains InAs QD in a GaAs matrix. It is designed to be single spatial mode with a shallow edged waveguide and a stripe width of  $w = 5$   $\mu\text{m}$ . One facet of the QDL diode is AR coated while the other is HR coated. The laser is mounted on a C-mount and the temperature is controlled by a Peltier element. The temperature is kept fixed to 10 °C. The emission wavelength is then centered at  $\lambda = 1225$  nm.

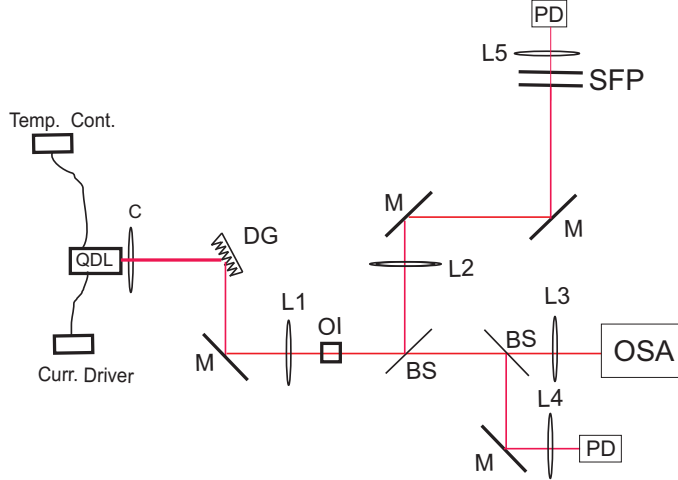


Figure 1. Experimental setup: quantum dot laser (QDL), aspheric collimator (C) ( $f = 3.1$  mm), diffraction grating (DG), mirror (M), L1 ( $f = 100$  mm), optical isolator (OI), beam splitter (BS), L2 ( $f = 250$  mm), scanning Fabry Perot interferometer (SFP), L3 ( $f = 35$  mm), L4 ( $f = 50$  mm), L5 ( $f = 50$  mm), optical spectrum analyzer (OSA), photo diode (PD).

The experimental setup is illustrated in Fig. 1. The emission in the fast axis is nearly collimated using a spherical lens (C) of 3.1 mm focal length and numerical aperture  $NA = 0.68$ . Feedback is provided in a Littrow scheme with a diffraction grating with 1450 lines/mm arranged at an angle  $\Theta = 75^\circ$  with respect to the incoming beam. The collimator is positioned in a way to optimize threshold reduction by focusing on the grating (external cavity length 123 mm). After the external cavity, there are two lenses L1, L2 for beam shaping and an optical isolator (OI) to prevent feedback from the detection part. Two InGaAs fast detector (Thorlabs PDA255) with an active area of 1 mm and bandwidth of 50 MHz are used to monitor the dynamics of the total intensity and the spectrally resolved intensity after the scanning Fabry-Perot interferometer (SFP). The optical spectrum is also monitored by a commercial fiber coupled optical spectrum analyzer (Agilent 86140) with a nominal resolution of 0.07 nm. The plane-plane scanning Fabry-Perot interferometer (SFP) has a free spectral range of 1.95 nm (390 GHz) and a finesse of about 500-600. For the characterization of the free running laser we simply replace the grating by a high reflectivity mirror.

The threshold current of the free running laser is  $I = 760$  mA. With feedback at the same wavelength ( $\lambda = 1225$ , gain peak) it is reduced to  $I = 550$  mA, a threshold reduction by 33%.

## 3. PHENOMENOLOGY OF SELF-PULSING

### 3.1 Experimental results

The free running laser shows strong pulsations according to Fig. 2 in a wide range of drive currents. The main polarization component is the horizontal, which is the one shown in Fig. 2, while the vertical polarization has about 10 times lower intensity but exhibits qualitatively the same behavior. The pulsations start around the threshold of the laser (Fig. 2(a)). They are large amplitude pulses on a small background. With increasing drive current their frequency increases, reaches a maximum (Fig. 2(b)), and then decreases again as is possible to see from Fig. 2(c). Fig. 2(b) is characterized by approximately 50% duty cycle. At higher currents, the on-state

dominates until the pulses are better described as short drop-outs from a high-amplitude state (Fig. 2(d)). The pulsations disappear after  $I = 850$  mA (Fig. 2(d)) and the laser emission is stable afterwards. It is evident from the figures that there is some variation in pulse duration (e.g. Fig. 2(c), (d)), i.e. there is a jitter in the width of the pulse present at all drive currents. Fig. 2(e) gives a quantitative account of the frequency of this pulsations

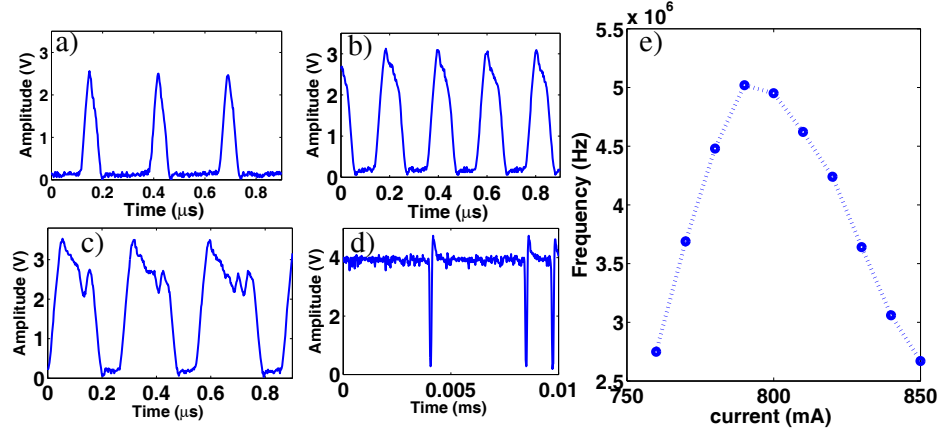


Figure 2. Behavior of the oscillation for the free running laser for increasing current: (a) threshold 760 mA, (b) 790 mA, (c) 830 mA, (d) 850 mA. (e) Frequency behavior of the free running laser for increasing current.

vs. drive current. The frequency of the pulsation starting at a current of 760 mA is about 2.75 MHz, reaches a maximum of 5.1 MHz for 790 mA, and then decreases again to 2.74 MHz at 850 mA.

The laser with feedback also shows oscillations as evidenced in Fig. 3. In this case the oscillations are more of a square-shape type. They appear at frequencies somewhat lower than the one in the free running laser and are centered around 1 MHz. Figs. 3(a)-(d) illustrate the development of pulsing in dependence of power. It is taken for lower emission wavelengths ( $\lambda = 1195$  nm) than the gain maximum but the qualitative behavior does not depend on wavelength and is quite the same as in the free-running laser: Short pulses from an off-state (not shown) evolve towards a 50% duty cycle (Fig. 3(a)). Then the on-phases become longer (Figs. 3(b) and (c)) until the laser is stable at high currents (Fig. 3(d))

Fig. 3(e) shows the range of the oscillation for different wavelengths available by tuning the diffraction grating from 1195 nm to 1250 nm. Between 1195 nm and 1220 nm the range where the oscillation are present is quite small, around 40 mA, then it increases to around 100 mA around the central wavelength to increase again up to 200 mA for some higher wavelength. This range is for both polarizations of the diode. The shape of the pulsation became less square-wave like for increasing wavelength (not shown in the picture).

Increasing the temperature results in the frequency of the oscillations becoming lower and the oscillation appear at higher current due to the shifting of the threshold of the laser with temperature.

### 3.2 Discussion

We note that we did not observe indications for higher QD state lasing as in<sup>9</sup> and the frequency of self-pulsing is in the MHz instead of the GHz range. The slow time scale of these oscillation indicates that these are opto-thermal pulsations. Opto-thermal pulsation are a common scenario in broad area semiconductor (quantum well) optical amplifiers though at slightly slower time scales of kHz to hundreds of kHz.<sup>1, 10</sup> The described phenomenology of pulsing from low-amplitude state vs. 50% duty cycle to drop-outs from a high-amplitude state is found nearly identically in both systems. In the amplifier, the scenario can be dynamically interpreted within the scenario of the van der Pol-Fitzugh-Nagumo model of interaction of dynamics at two very different time scales. In physical terms, there is a competition between two frequencies/resonances, e.g. in a laser with injection the frequency of the injected light and the cavity resonance of the slave. Initially they might be in resonance but if

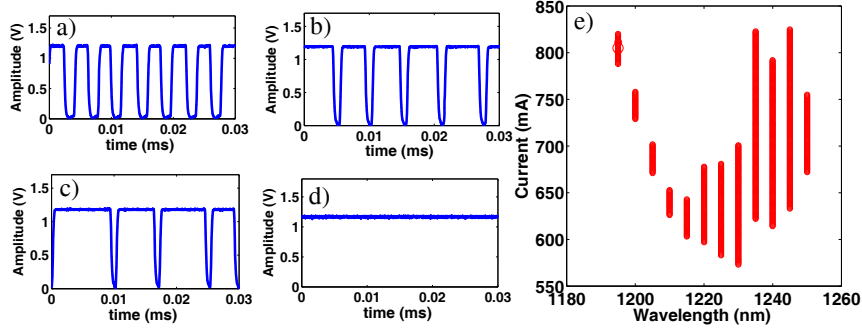


Figure 3. Evolution of oscillation for increasing current at: (a)  $\lambda = 1195$  nm 790 mA (b) 810 mA (c) 820 mA and (d) 830 mA (e) Oscillation range in dependence of wavelength.

then amplification sets in, the slave cools due to the reduction in carrier density due to stimulated emission, its resonance shifts and interaction is lost. Then the carrier density is high again and the laser heats until it is in resonance again and a new pulse can start. The different time scales of thermal heating/cooling and stimulated emission/carrier injection lead then to relaxation oscillation-like pulsations. The same might happen in an experiment with frequency-selective feedback into a single-longitudinal mode vertical-cavity surface-emitting laser (VCSEL) where the role of the injection frequency is played by the center frequency of the grating.<sup>17</sup>

The difference between our case and the previous cited literature is the fact that in our case these oscillations appear also in the free running lasers. This indicates that the laser itself provides a mechanism able to generate oscillations in the MHz range. Current investigations address differences between the dynamics in device center and beam wings, which might indicate thermal lensing or waveguiding in maintaining the pulsations. This, and the fact that one is interested in a direct proof for a transient temperature shift during the pulse motivates an investigation of the optical spectra, especially time-resolved ones.

## 4. TIME-RESOLVED SPECTRA

### 4.1 Experimental results

Fig. 4 shows standard time-averaged spectra (i.e. the sweeping time of the SFP is much longer than the time scale of pulsations) around the gain peak ( $\lambda = 1220$  nm) for two cases, both with feedback, when the laser is not oscillating, upper part (a), and when the laser exhibits oscillations, lower one (b). In both cases, the laser is strongly multi-mode covering about 1.5 nm. The modal envelope is increasing from lower to higher wavelengths. The line width of an individual longitudinal mode is about 0.6 GHz for stable emission. Instead, when pulsating the average linewidth is larger (Fig. 4b), about 5.6 GHz, which might be due to modes jittering.

Following,<sup>18</sup> we then record the time-resolved spectrum for all frequencies inside a free spectral range and superimpose the data recorded for every frequency. This is done by scanning the piezoelectric translators of the SFP by a computer controlled voltage slowly (stepwise) while we record with a fast detector the signal transmitted by the SFP. The diode drive current is kept fixed during the experiment. To maintain a stable signal on the scope we trigger on the pulse read out by the other fast detector. In our case 0.47 V correspond to a free spectral range of 1.95 nm. The scan covers 0.8 V with a resolution of 1 mV steps leading to almost two FSR with a nominal wavelength resolution of 0.0041 nm.

Fig. 5 shows the time-resolved spectra for two different wavelength achievable tuning the diffraction grating. Fig. 5(a) is for  $\lambda = 1197$  nm at  $I = 724$  mA, almost at the low-wavelength edge of the tuning range. One can see that the trajectory of each longitudinal mode is initially curved (blue-shifting) until it remains essentially constant for the remainder of the pulse. This blue-shift covers about 0.13 nm and might be due to radiative

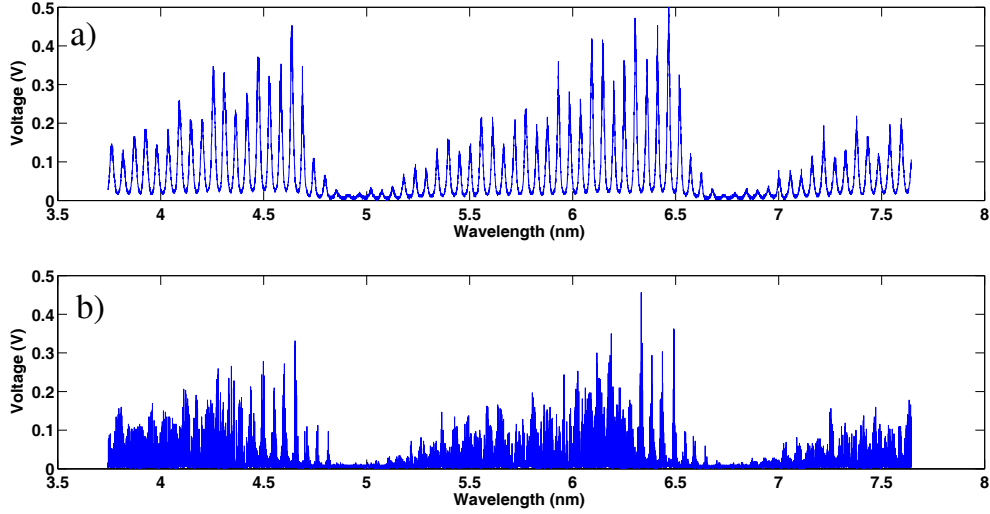


Figure 4. Time-averaged spectra for two relevant currents: (a) laser stable at  $I = 584$  mA, (b) laser oscillating at  $I = 548$  mA. The wavelength scale is only relative, the free spectral range of the analyzing SFP is 1.95 nm, i.e. the repetition of modes is a detection artefact.

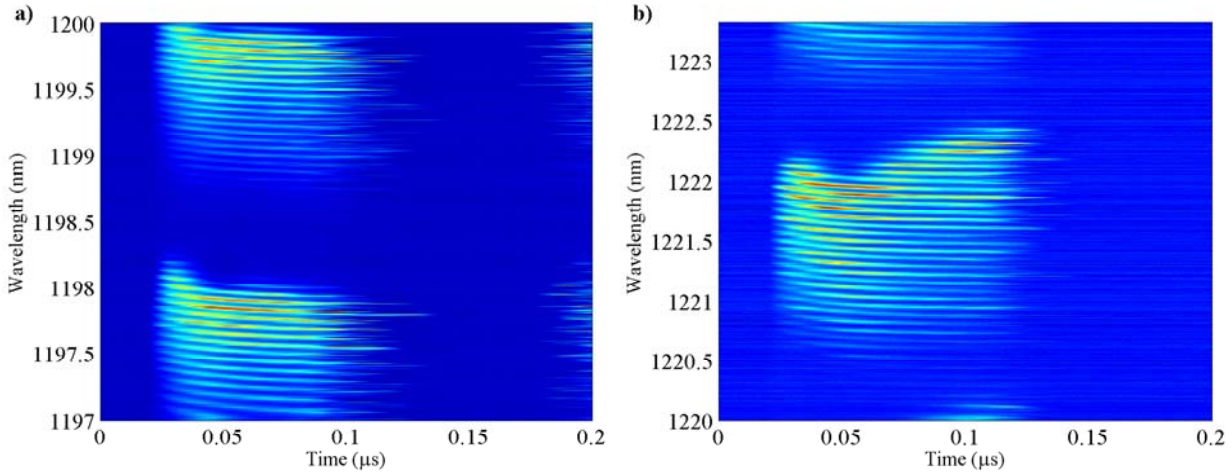


Figure 5. Time-resolved spectrum for (a)  $\lambda = 1197$  nm,  $I = 724$  mA, (b)  $\lambda = 1220$  nm,  $I = 548$  mA.

cooling. This would fit the interpretation in the amplifier systems<sup>19</sup> where it wasn't demonstrated experimentally explicitly though. In addition, the envelope of lasing also blue-shifts with the most reddish modes dying first.

Fig. 5(b) is for  $\lambda = 1220$  nm, around the gain peak, at  $I = 548$  mA. Again the envelope blue-shifts in the initial phase but then swings back towards the red. Within each cavity mode there is a blue-shift of 0.11 nm.

Fig. 6(a) is for  $\lambda = 1240$  nm at  $I = 600$  mA. In this case, the lasing starts at low wavelengths and then the envelope red-shifts. Within each cavity mode there is a blue-shift of 0.06 nm.

Fig 6(b) shows instead the time-resolved spectrum for the free running laser at a typical current. In this case there is a very weak blue-shift of 0.02 nm for each longitudinal mode but the envelope does not shift very much. The fact that the diagram is quite jagged for longer times is related to the fact that there is a larger dispersion of pulse length in the free-running laser than in the laser with feedback which makes the sampling technique less reliable further away from the trigger point.

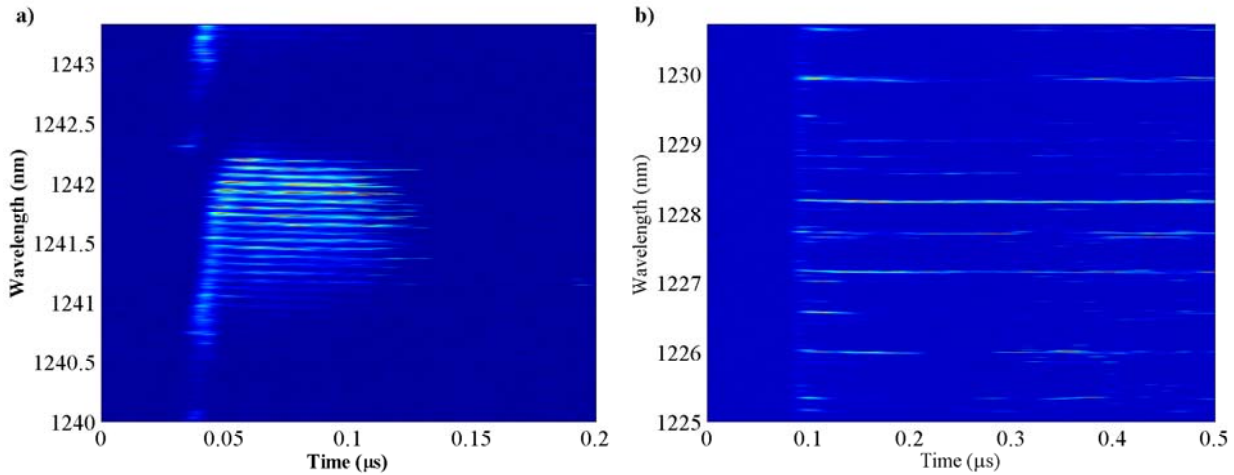


Figure 6. Time resolved spectrum for (a)  $\lambda = 1240$  nm at  $I = 600$  mA, (b) free running laser,  $\lambda = 1225$  nm,  $I = 831$  mA. In b) the FSR of the analyzing SFP was increased to 5.7 nm

## 4.2 Discussion

Switching between longitudinal modes was discussed in<sup>20–23</sup> for quantum well lasers and in<sup>24</sup> for quantum dot lasers. An important conclusion was that longitudinal mode switching is not a merely stochastic process but follows a quite deterministic switching sequence influenced by nonlinearities. A preference for a switching sequence from blue to red modes was related to the breaking of the symmetry of four-wave mixing processes by a nonzero alpha-factor. The alpha-factor or linewidth-enhancement factor describes phase-amplitude coupling in semiconductors and is positive for quantum well samples.<sup>25</sup> It is related to the fact that the gain spectrum (imaginary part of susceptibility) of quantum wells is asymmetric and as a consequence its Hilbert transform giving the real part (refractive index) contribution is not zero at gain maximum. A positive  $\alpha$ -factor was found to be consistent with the blue-to-red switching sequence observed.<sup>21,23</sup> The 3D quantum confinement of ideal QD should lead to a ‘quasi-atomic’ behavior with a delta function-like density of states. A symmetric asymmetric gain spectrum should have zero phase-amplitude coupling or linewidth enhancement factor at gain maximum, positive for lower frequencies and negative for higher frequencies. The different shift of the longitudinal modes during the pulses observed is in qualitative agreement with this expectation: On gain maximum, the free-running as well as the laser with feedback do not show much of a shift consistent with a zero or small alpha-factor. The detuned emission under frequency-selective feedback shows the same tendency as the quantum well devices for lower frequencies (positive alpha-factor) and the opposite for higher frequencies (negative alpha-factor). The size and sign of the alpha-factor is very important for feedback and filamentation instabilities. Indeed, a reduced (or even negative)  $\alpha$ -factor and a reduced tendency to beam filamentation was observed in many QD samples, at least under some operating conditions.<sup>26–31</sup> The real susceptibility of QD are more complicated than the one of a two-level atom due to contributions from the wetting layer, higher QD states and inhomogeneous broadening (e.g.<sup>32</sup>), though the possibility of a negative  $\alpha$ -factor under gain conditions can survive. The current observation of a qualitative agreement with the two-level expectation seems to be interesting though it should be cautioned that the argument is quite indirect.

Finally, the fact that each longitudinal mode blue-shifts at the beginning of the pulse hints to a detuning-independent effect like a temperature shift. Indeed, it is consistent with radiative cooling, which might trigger the thermal relaxation oscillations.

## 5. CONCLUSION

Self-sustained pulsations of the output have been observed in a InAs quantum dot laser diode in the MHz range for the first time. The pulsations have in tendency a square-wave-like appearance and are present for a wide range of current and wavelength. The free-running laser and the laser with feedback show qualitatively the same

behavior except in frequency-resolved optical spectra. Here the different shift of the envelope might be related to a change of phase-amplitude coupling across the gain maximum in qualitative agreement with the expectation for a general two level system. The time scale and the bifurcation scenario suggest that these are opto-thermal pulsations like the ones reported in quantum well amplifiers<sup>1</sup> but there is no obvious mechanism of a competition between resonance conditions. Instead, we are currently investigating the hypothesis of a dynamical change of thermal waveguiding properties.

### Acknowledgements

This work was supported by EPSRC project EP/E025021. We are grateful for useful discussions with Daniil Livshits from Innolume GmbH.

### REFERENCES

- [1] Barland, S., Piro, O., Giudici, M., Tredicce, J. R., and Balle, S., “Experimental evidence of van der Pol-Fitzhugh-Nagumo dynamics in semiconductor optical amplifiers,” *Phys. Rev. E* **68**, 036209 (2003).
- [2] Bhattacharya, P., Bimberg, D., and Arakawa, Y., “Special issue on optoelectronic devices based on quantum dots,” *Proc. IEEE* **95**, 1718–1722 (2007).
- [3] Sugawara, M. and Usami, M., “Quantum dot devices: Handling the heat,” *Nature Phot.* **3**, 30–32 (2009).
- [4] Qasaimeh, O., Zhou, W.-D., Phillips, J., Krishna, S., Bhattacharyaa, P., and Dutta, M., “Bistability and self-pulsation in quantum-dot lasers with intracavity quantum-dot saturable absorbers,” *Appl. Phys. Lett.* **74**, 1654–1657 (1999).
- [5] Summers, H. D., Matthews, D. R., Smowton, P. M., Rees, P., and Hopkinson, M., “Laser dynamics in self-pulsating quantum dot systems,” *J. Appl. Phys.* **95**, 1036–1042 (2004).
- [6] Viktorov, E. A., Cataluna, M. A., OFaolain, L., Krauss, T. F., Sibbett, W., Rafailov, E. U., and Mandela, P., “Dynamics of a two-state quantum dot laser with saturable absorber,” *Appl. Phys. Lett.* **90**, 121113 (2007).
- [7] Liu, H., Smowton, P., Summers, H., Edwards, G., and Drexler, W., “Self-pulsing 1050 nm quantum dot edge emitting laser diodes,” *Appl. Phys. Lett.* **95**, 101111 (2009).
- [8] Kuzmenkov, A. G., Ustinov, V. M., Sokolovskii, G. S., Maleev, N. A., Blokhin, S. A., Deryagin, A. G., Chumak, S. V., Shulenkov, A. S., Mikhrin, S. S., Kovsh, A. R., McRobbie, A. D., Sibbett, W., Cataluna, M. A., and Rafailov, E. U., “Self-sustained pulsation in the oxide-confined vertical-cavity surface-emitting lasers based on submonolayer InGaAs quantum dots,” *Appl. Phys. Lett.* **91**, 121106 (2007).
- [9] Mokkaapati, S., Tan, H. H., Jagadish, C., and Buda, M., “Self-sustained output power pulsations in InGaAs quantum dot ridge-waveguide lasers,” *Appl. Phys. Lett.* **92**, 021104 (2008).
- [10] Marino, F., Catalán, G., Sánchez, P., Balle, S., and Piro, O., “Thermo-optical canard orbits and excitable limit cycles,” *Phys. Rev. Lett.* **92**, 073901 (2004).
- [11] Wegener, M. and Klingshirn, C., “Self-oscillations of an induced absorber (CdS) in a hybrid ring resonator,” *Phys. Rev. A* **35**, 1740–1752 (1987).
- [12] Rzhanov, Y. A., Richardson, H., Hagberg, A. A., and Moloney, J. V., “Spatiotemporal oscillations in a semiconductor etalon,” *Phys. Rev. A* **47**, 1480–1491 (1993).
- [13] Lu, W., Yu, D., and Harrison, R. G., “Excitability in a nonlinear optical cavity,” *Phys. Rev. A* **58**, R809–R811 (1998).
- [14] Suret, P., Derozier, D., Lefranc, M., Zemmouri, J., and Bielawski, S., “Self-pulsing instabilities in an optical parametric oscillator: Experimental observation and modeling of the mechanism,” *Phys. Rev. A* **61**, 021805(R) (2000).
- [15] FitzHugh, R., “Impulses and physiological states in theoretical models of nerve membrane,” *Biophys. J.* **1**, 445–466 (1961).
- [16] Nagumo, J. S., Arimoto, S., and Yoshizawa, S., “An active pulse transmission line simulating nerve axon,” *Proc. IRE* **50**, 2061–2070 (1962).
- [17] Ackemann, T., Barland, S., Balle, S., and Tredicce, J. R. (1999). Unpublished.

- [18] Huyet, G., Balle, S., Giudici, M., Green, C., Giacomelli, G., and Tredicce, J. R., “Low frequency fluctuations and multimode operation of a semiconductor laser with optical feedback,” *Opt. Commun.* **149**, 341–347 (1998).
- [19] Barland, S., Tredicce, J. R., Brambilla, M., Lugiato, L. A., Balle, S., Giudici, M., Maggipinto, T., Spinelli, L., Tissoni, G., Knödel, T., Miller, M., and Jäger, R., “Cavity solitons as pixels in semiconductors,” *Nature* **419**, 699–702 (2002).
- [20] Ahmed, M. and Yamada, M., “Influence of instantaneous mode competition on the dynamics of semiconductor lasers,” *IEEE J. Quantum Electron.* **38**(6), 682–693 (2002).
- [21] Yamada, M., Ishimori, W., Sakaguchi, H., and Ahmed, M., “Time-dependent measurement of the mode-competition phenomena among longitudinal modes in long-wavelength lasers,” *IEEE J. Quantum Electron.* **39**, 1548–1555 (2003).
- [22] Furfaro, L., Pedaci, F., Giudici, M., Hachair, X., Tredicce, J., and Balle, S., “Mode-switching in semiconductor lasers,” *IEEE J. Quantum Electron.* **40**, 1365 (2004).
- [23] Yacomotti, A. M., Furfaro, L., Hachair, X., Pedaci, F., Giudici, M., Tredicce, J. R., Javaloyes, J., Balle, S., Viktorov, E. A., and Mandel, P., “Dynamics of multimode semiconductor lasers,” *Phys. Rev. A* **69**, 053816 (2004).
- [24] Tanguy, Y., Houlihan, J., Huyet, G., Viktorov, E. A., and Mandel, P., “Synchronization and clustering in a multimode quantum dot laser,” *Phys. Rev. Lett.* **96**, 053902 (2006).
- [25] Henry, C. H., “Theory of the linewidth of semiconductor lasers,” *IEEE J. Quantum Electron.* **18**, 259–264 (1982).
- [26] Bimberg, D. and Ledentsov, N. N., “Quantum dots: lasers and amplifiers,” *J. Phys.: Condens. Matter* **15**, R1063–R1076 (2003).
- [27] Smowton, P. M., Pearce, E. J., Schneider, H. C., Chow, W. W., and Hopkinson, M., “Filamentation and linewidth enhancement factor in InGaAs quantum dot lasers,” *Appl. Phys. Lett.* **81**, 3251–3253 (2002).
- [28] Xu, Z., Birkedal, D., Juhl, M., and Hvam, J. M., “Submonolayer InGaAs/GaAs quantum-dot lasers with high modal gain and zero-linewidth enhancement factor,” *Appl. Phys. Lett.* **85**, 3259–3261 (2004).
- [29] Ribbat, C., Selin, R. L., Kaiander, I., Hopfer, F., Ledentsov, N. N., Bimberg, D., Kovsh, A. R., Ustinov, V. M., Zhukov, A. E., and Maximov, M. V., “Complete suppression of filamentation and superior beam quality in quantum-dot lasers,” *Appl. Phys. Lett.* **82**, 952–954 (2003).
- [30] Schneider, S., Borri, P., Langbein, W., Woggon, U., Sellin, R. L., Ouyang, D., and Bimberg, D., “Linewidth Enhancement Factor in InGaAs Quantum-Dot Amplifiers,” *IEEE J. Quantum Electron.* **40**, 1423–1429 (2004).
- [31] Hegarty, S. P., Corbett, B., McInerney, J. G., and Huyet, G., “Free-carrier effect on index change in 1.3  $\mu\text{m}$  quantum-dot lasers,” *Electron. Lett.* **41**, 416–418 (2005).
- [32] Schneider, H. C., Chow, W. W., and Koch, S. W., “Anomalous carrier-induced dispersion in quantum-dot active media,” *Phys. Rev. B* **66**, 041310(R) (2006).